

A VAN LEER SHOCK CAPTURING ALGORITHM FOR THE EULER EQUATIONS(U) ARMY BALLISTIC RESEARCH LAB ABERDEEN PROVING GROUND MD C H COOKE OCT 84 BRL-MR-3480

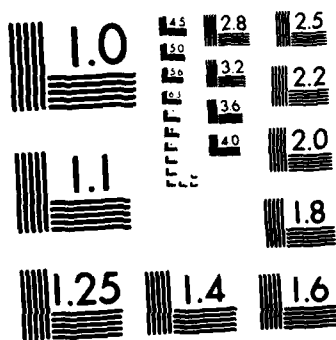
EQUATIONS FOR THE PROBABILISTIC RESEARCH LAB BERKELEY
PROVING GROUND MD C H COOKE OCT 84 BRL-MR-3400

SBI-AD-F300 513

F/G 20/4

ML

[illegible]



MICROCOPY RESOLUTION TEST CHART
NATIONAL BUREAU OF STANDARDS-1963-A

AD-A148 761

12

B
R
L

AD-F300 513

MEMORANDUM REPORT BRL-MR-3400

A VAN LEER SHOCK CAPTURING ALGORITHM
FOR THE EULER EQUATIONS

Charlie H. Cooke

October 1984

DTIC
ELECTE
DEC 7 1984
S B

DTIC FILE COPY

APPROVED FOR PUBLIC RELEASE; DISTRIBUTION UNLIMITED.

US ARMY BALLISTIC RESEARCH LABORATORY
ABERDEEN PROVING GROUND, MARYLAND

84 12 04 101

Destroy this report when it is no longer needed.
Do not return it to the originator.

Additional copies of this report may be obtained
from the National Technical Information Service,
U. S. Department of Commerce, Springfield, Virginia
22161.

The findings in this report are not to be construed as an official
Department of the Army position, unless so designated by other
authorized documents.

The use of trade names or manufacturers' names in this report
does not constitute indorsement of any commercial product.

SECURITY CLASSIFICATION OF THIS PAGE (When Data Entered)

DD FORM 1 JAN 73 1473 EDITION OF 1 NOV 68 IS OBSOLETE

SECURITY CLASSIFICATION OF THIS PAGE (When Data Entered)

TABLE OF CONTENTS

	<u>Page</u>
LIST OF ILLUSTRATIONS.	5
I. INTRODUCTION	7
II. GOVERNING EQUATIONS.	9
III. GODUNOV METHODS.	10
A. First-Order Accurate Method.	11
B. Second Order Method.	12
C. Resolved Interface Initial Time Derivatives.	14
IV. COMPUTATIONAL RESULTS.	15
Table 1. Linear Shock Tube Data	15
V. SUMMARY AND CONCLUSIONS.	16
REFERENCES	31
DISTRIBUTION LIST.	33



Accession For	
NTIS GRA&I	<input checked="checked" type="checkbox"/>
DTIC TAB	<input type="checkbox"/>
Unannounced	<input type="checkbox"/>
Justification	
By	
Distribution/	
Availability Codes	
Dist	Avail and/or Special
A-1	

LIST OF ILLUSTRATIONS

<u>Figure</u>		<u>Page</u>
1	Two-Dimensional, Axis-Symmetric Muzzle Blast Calculation. . . .	18
2	Shock Smearing Typical of a First Order Accurate Godunov Calculation	19
3	First Order Godunov Calculation	20
4	First Order Godunov Calculation	21
5	First Order Godunov Calculation	22
6	First Order Godunov Calculation	23
7	Second Order Godunov Calculation.	24
8	Second Order Godunov Calculation.	25
9	Second Order Godunov Calculation.	26
10	Second Order Godunov Calculation.	27
11	Progression of Pressure Jump, Second Order Godunov.	28
12	Progression of Velocity Jump, Second Order Godunov.	29

I. INTRODUCTION

A current focus of interest in the U.S. Army ballistic research program involves the numerical calculation of compressible flow about muzzle brake devices. By absorbing a portion of the recoil impulse, the muzzle brake permits design of large caliber weapons characterized by increased range without increased weight. Near field calculations are helpful in studying fatigue life and structural integrity of blast-loaded surfaces. Far-field calculations, which often can be performed with less complex flow models, can determine if safe maximum overpressures exist in the gun crew area.

Near-to-intermediate range muzzle brake calculations have recently been obtained¹ using a popular, locally one-dimensional, first-order accurate method of Godunov.² Model results afford predictions of peak over-pressure levels in the proximity of the brake and provide initial data for continuing far-field calculations by independent means.

In the interest of economizing computer resources, for far-field calculations, it is desirable to employ simple one-dimensional flow models. Mach contours for the early stages of a typical blast are exhibited in Figure 1. Already, local spherical symmetry is suggested, and evidence from spark photography confirms that the trend is characteristic of later evolution.¹ Under this hypothesis, some exploratory far-field calculations are underway, which utilize spherically symmetric flow models and the numerical method of characteristics.^{3,4}

1. G. E. Widhopf, J. C. Buell, and E. M. Schmidt, "Time Dependent Near-Field Muzzle Brake Simulations," AIAA-82-0973, AIAA/ASME 3rd Joint Thermophysics, Fluids and Heat Transfer Conference, St. Louis, Missouri, June 1982.
2. A. M. Godunov, A. V. Zabrodin, and G. P. Prokopov, "Difference Schemes for Two-Dimensional, Unsteady Problems in Gas Dynamics and Calculation of Flows With a Detached Shock Wave," Journal of Computing Mathematics and Mathematical Physics, USSR Academy of Sciences, Vol. 1, No. 6, November - December 1961. (Translation)
3. M. L. Bundy, "A Nonsimilar Solution for Blast Waves Driven by an Asymptotic Piston Expansion," AIAA-83-0496, AIAA 21st Aerospace Sciences Meeting, January 1983, Reno, Nevada and U. S. Army Ballistic Research Laboratory, Aberdeen Proving Ground, MD, BRL Technical Report ARBRL-TR-02497, June 1983. (AD A130012)
4. M. L. Bundy, C. H. Cooke, and E. M. Schmidt, "Reshaping an Artificially Diffused Shock Solution," BRL Report, to be published.

The objective of the present research is to investigate an alternative numerical method, which might complement, or perhaps supplant, the method of characteristics approach. Our intent is to revise Van Leer's second-order accurate, Godunov method,⁵ originally formulated in the framework of Lagrangean fluid dynamics, for application to the one-dimensional Euler equations. A similar effort, as yet unpublished, and which differs somewhat in philosophy, has been carried out by Colella.⁶

The desirability of investigating second-order accurate methods for shock capturing is illustrated by Figure 2. Here, the first-order Godunov method, implemented by personnel of Aerospace Corporation for numerical solution of the two-dimensional axis-symmetric Euler equations, has been applied to calculate a conical flow which simulates some of the more dominant characteristics of a muzzle blast. Assuming there is provided some heuristic model of contact surface history, as well as initial data between the outer shock and its driving contact surface, this calculation could be continued into the far-field by the method of characteristics.³ However, shock smearing due to the artificial viscosity of the numerical method in this case makes troublesome the question of precise shock location and strength. A reshaping of initial data near the shock, or else a more accurate calculation which provides crisper shock structure, appears to be called for.

In the past few years, a variety of new methods for numerical calculation of flows with embedded shocks has evolved, of which references 5-9 are perhaps a representative sample. Van Leer's second-order sequel to the original Godunov method appears among the more promising. The method is alledged⁵ to give

-
5. B. Van Leer, "Towards The Ultimate Conservative Difference Scheme. V. A Second-Order Sequel to Godunov's Method," Journal of Computational Physics, Vol. 32, pp. 101-136, 1979.
 6. P. Colella, "A Direct Eulerian MUSCL Scheme for Gas Dynamics," Lawrence Berkeley Laboratory Report LBL-14104, February 1982.
 7. J. L. Steger and W. F. Warming, "Flux Vector Splitting of the Inviscid Gas Dynamics Equations with Application To Finite Difference Methods," Journal of Computational Physics, Vol. 40, No. 2, April 1981.
 8. G. Moretti, "The λ Scheme," Computers and Fluids, Vol. 7, pp. 191-205, Pergamon Press, 1979.
 9. H. C. Yee and R. J. Warming, "Implicit Total Variation Diminishing Schemes For Steady Flow Calculations," AIAA-83-1902, AIAA 6th Computational Fluid Dynamics Conference, Danvers, Massachusetts, July 1983.

superior resolution of shocks and flow discontinuities, compared, say, to the methods surveyed by Sod¹⁰ and Miner and Skop.¹¹ However, remapping from the Lagrangean to Euler variables requires, perhaps significant, extended computing time per cycle.⁵ Hence, it appears an unnecessary encumbrance.

The purpose, then, of this research is to reformulate Van Leer's algorithm in Eulerian fluid dynamics framework, revising as it becomes necessary, in order to achieve a more accurate, one-dimensional shock capturing algorithm, which could also be employed in two-dimensional calculations through fractional splitting of the equations of flow.⁵

II. GOVERNING EQUATIONS

In strong conservation law form, the Euler equations for one-dimensional ideal compressible flow can be written

$$\frac{\partial U}{\partial t} + \frac{\partial F}{\partial R} + G = 0. \quad (1)$$

Here

$$U = \begin{bmatrix} \rho \\ \rho u \\ \rho E \end{bmatrix} \quad F = \begin{bmatrix} \rho u \\ P + \rho u^2 \\ (P + \rho E)u \end{bmatrix} \quad G = \frac{\sigma}{R} \begin{bmatrix} \rho u \\ \rho u^2 \\ (P + \rho E)u \end{bmatrix} \quad (2)$$

where $\sigma = 0, 1$, or 2 , in turn for cartesian, cylindrical, or spherical coordinates. R is the respective distance coordinate.

The fluid dynamic variables are:

c = local speed of sound in fluid

ρ = density

u = velocity

-
10. G. A. Sod, "A Survey of Several Finite Difference Methods For Systems of Hyperbolic Conservation Laws," Journal of Computational Physics, Vol. 27, pp. 1-31, 1978.
 11. E. W. Miner and R. A. Skop, "Explicit Time Integration For The Finite Element Shock Wave Equations," AIAA-82-0994, ASME/AIAA 3rd Joint Thermophysics, Fluids, Plasma and Heat Transfer Conference, St. Louis, Missouri, June 1982.

p = pressure

E = specific total energy

e = specific internal energy.

Here c_p, c_v are specific heats, and

$$\gamma = c_p / c_v$$

$$c^2 = \gamma P / \rho$$

$$P = (\gamma - 1) \rho e$$

$$E = e + \frac{u^2}{2}.$$

III. GODUNOV METHODS

We shall derive the Godunov algorithm for the case of a uniform grid; however, the method is readily adaptable to encompass non-uniformity. By integrating Equation (1) over a typical space-time cell $R_i \leq R \leq R_{i+1}$; $t_n < t < t_{n+1}$ and applying Green's theorem for the plane, we arrive at the exact equation

$$\bar{U}^{i+1/2} = \bar{U}_{i+1/2} - \frac{\Delta t}{\Delta R} \langle F \rangle \left|_i^{i+1} - \frac{1}{\Delta R} \int_{t_n}^{t_{n+1}} \int_{R_i}^{R_{i+1}} G \, dR \, dt. \quad (3)$$

Here, superscript usage of a space index denotes advanced time level, while corresponding subscript usage denotes present time level: i.e.,

$$(\)^i = (\)_{i,n+1} \quad (4)$$

$$(\)_i = (\)_{i,n}.$$

The space average over a cell, space-centered at $R_{i+1/2}$, is

$$\bar{U}_{i+1/2} = \frac{1}{\Delta R} \int_{R_i}^{R_{i+1}} U(R, t_n) \, dR, \quad \Delta R = R_{i+1} - R_i; \quad (5)$$

while the time average flux on interface $R = R_i$ is

$$\langle F \rangle_i = \frac{1}{\Delta t} \int_{t_n}^{t_{n+1}} F(U(R_i, t)) dt, \quad \Delta t = t_{n+1} - t_n. \quad (6)$$

Godunov's method can be made first- or second-order accurate, depending upon how the flux integrals, Equation (6) and the cell integral of G in Equation (3) are approximated.

A. First-Order Accurate Method

In Godunov's original derivation,² the function $U(R, t_n)$ is approximated with a piecewise constant function which on cell $R_i \leq R \leq R_{i+1}$ assumes the average value $\bar{U}_{i+1/2}$. Cell averages are updated to the next time level through approximating the integrals in Equation (3), by solving a Riemann problem at each cell interface. The Riemann problem entails the solution of Equation (1) for $t > t_n$, with $\sigma = 0$ and with initial conditions at $t = t_n$ given by:

$$V = \begin{cases} \bar{V}_{i+1/2}, & R > R_i \\ \bar{V}_{i-1/2}, & R < R_i \end{cases} \quad (7)$$

where $V^T = (P, \rho, u)$. However, only the resulting values of V on the interface R_i are of interest. The primary mechanism for interaction of the discontinuity, Equation (7), is the propagation of expansion or compression waves away from the interface. The nonlinear equations which afford an iterative solution of the Riemann problem are well-documented in references 5, 10, and 12.

For purposes of numerical stability, the time step Δt is chosen to be such that propagation times are insufficient to allow waves from adjacent discontinuities to have influence on interface $R = R_i$. Then values

$$V_i^* = \lim_{t \rightarrow t_n^+} V(R_i, t) \quad (8)$$

12. M. Holt, Numerical Fluid Dynamics, Springer-Verlag, Berlin, Heidelberg, New York, 1977.

obtained from solving the Riemann problem at each interface, together with cell average values, are used to approximate the integrals in Equation (3). Godunov's first-order accurate method results:

$$\bar{U}^{i + \frac{1}{2}} = \bar{U}_{i + \frac{1}{2}} - \frac{\Delta t}{\Delta R} [F(U_{i + 1}^*) - F(U_i^*)] - \Delta t G(\bar{U}_{i + \frac{1}{2}}). \quad (9)$$

B. Second Order Method

For the second-order accurate Godunov method, primitive quantities stored at each time level are cell average $\bar{U}_{i + \frac{1}{2}}$ and interface differences $[V]_{i + \frac{1}{2}} = V_{i + 1} - V_i$. The calculation of the average derivative is now possible:

$$(\bar{V}_R)_{i + \frac{1}{2}} = \frac{\partial \bar{V}}{\partial R}_{i + \frac{1}{2}} = \frac{1}{\Delta R} \int_{R_i}^{R_{i + 1}} \frac{\partial V}{\partial R} dR = \frac{[V]_{i + \frac{1}{2}}}{\Delta R}. \quad (10)$$

This affords a more accurate, piecewise linear function approximation: On a cell $R_i \leq R \leq R_{i + 1}$,

$$V = \bar{V}_{i + \frac{1}{2}} + (\bar{V}_R)_{i + \frac{1}{2}} (R - R_{i + \frac{1}{2}}). \quad (11)$$

Corresponding inputs for the Riemann problem at interface R_i are, from Equation (11),

$$V_{i \pm} = \bar{V}_{i \pm \frac{1}{2}} \mp \frac{1}{2} [V]_{i \pm \frac{1}{2}}. \quad (12)$$

The output from the Riemann problem, solved as previously, is the value

$$V_i^* = \lim_{t \rightarrow t_n^+} V(R_i, t), \quad (13)$$

which results immediately after the interface discontinuity is resolved. In addition, a value

$$V_t^* = \lim_{t \rightarrow t_n^+} \frac{\partial V}{\partial t} (R_i, t) \quad (14)$$

for the corresponding resolved time derivative is to be obtained by auxiliary

means (see next section). As established by Van Leer,¹ the interface approximation

$$V = V_i^* + (V_t)_i^* (t - t_n) + O(\Delta t)^2 \quad (15)$$

can be applied to evaluate, with a higher order of accuracy, the flux integrals in Equation (3). The cell integral can be approximated, employing the trapezoidal rule, with

$$\int_{t_n}^{t_{n+1}} \int_{R_i}^{R_{i+1}} G \, dR \, dt = \quad (16)$$

$$\frac{\Delta R}{2} \int_{t_n}^{t_{n+1}} [G(R_{i+1}, t) + G(R_i, t)] dt + O(\Delta R)^3$$

which now involves interface values. For a typical interface integral

$$\int_{t_n}^{t_{n+1}} G(U, R_i) dt = \frac{\Delta t}{2} [G(U_i^i, R_i) + G(U_i, R_i)] + O(\Delta t)^3. \quad (17)$$

Advanced time level interface values are predicted by means of

$$V^i = V_i^* + (V_t)_i^* \Delta t + O(\Delta t)^2, \quad (18)$$

and initial interface differences with

$$[V]^{i+\frac{1}{2}} = V^{i+1} - V^i. \quad (19)$$

At the cost of additional storage and altered processing stream, after solution of the Riemann problem adjusted interface differences

$$[V]_{i+\frac{1}{2}}^* = V_{i+1}^* - V_i^* \quad (20)$$

could be computed, to be used for more accurate evaluation of the interface time derivatives, described below. However, Van Leer does not appear to have used this device, and we have not verified whether the additional cost is justified.

C. Resolved Interface Initial Time Derivatives

For the compressible flow equations, Equations (1-2), compatibility relations along characteristics are,

$$\frac{dP}{dt} = c^2 \frac{d\rho}{dt} \quad (21)$$

$$\text{on } \frac{dR}{dt} = u$$

$$\frac{du}{dt} \pm \frac{1}{\rho c} \frac{dP}{dt} = \pm \frac{\sigma u c}{R} \quad (22)$$

$$\text{on } \frac{dR}{dt} = u \pm c.$$

To better insure correct transmission of signals, these Equations are differenced (spatially) as in Moretti's λ - scheme,⁸ in order to obtain relations which can be solved for initial interface time derivatives. This differencing is given by the equations

$$\frac{\partial u}{\partial t}_i^* + \left(\frac{1}{\rho c}\right)_i^* \left(\frac{\partial P}{\partial t}\right)_i^* = - (u + c)_{i+} \left\{ \frac{\partial u}{\partial R} + \frac{1}{\rho c} \frac{\partial P}{\partial R} \right\}_{i+} + \left(\frac{\sigma u c}{R}\right)_i^* \quad (23)$$

$$\frac{\partial u}{\partial t}_i^* - \left(\frac{1}{\rho c}\right)_i^* \left(\frac{\partial P}{\partial t}\right)_i^* = - (u - c)_{i-} \left\{ \frac{\partial u}{\partial R} - \frac{1}{\rho c} \frac{\partial P}{\partial R} \right\}_{i-} - \left(\frac{\sigma u c}{R}\right)_i^* \quad (24)$$

$$\frac{\partial \rho}{\partial t}_i^* = \frac{1}{(c^*)_i^2} \left\{ \frac{\partial P}{\partial t}_i^* + (u \frac{\partial P}{\partial R})_{i+} \right\} - (u \frac{\partial \rho}{\partial R})_{i+} \quad (25)$$

Where space derivative occur in Equations (23-29), average space derivatives are used, on the (+) side of an interface. Depending upon whether or not u is positive, up- or down-wind differencing is employed in Equation (25).

IV. COMPUTATIONAL RESULTS

The first and second-order Godunov methods previously discussed have been applied to the linear shock tube calculation reported by Miner and Skop.¹¹ Here, an infinite tube contains gas in two compartments initially separated by a diaphragm. Table I shows the respective initial conditions.

TABLE 1. LINEAR SHOCK TUBE DATA

$P_0 = 1.$	$P_1 = .1$
$\rho_0 = 1.$	$\rho_1 = .125$
$u_0 = 0.$	$u_1 = 0.$

The Godunov calculation is programmed to choose its own time step, in accordance with stepwise stability restrictions. The results after one hundred cycles, for the first-order accurate calculation, are displayed in Figures 3-6. Figures 4-5, in particular, show the smearing of shock structure due to the inherent numerical dissipation of the method, present even on this very fine grid.

The second-order accurate method is activated by a program switch. Figures 7-10 show the results after another one hundred cycles of calculation. An immediate sharpening of the shock is to be observed.

It seems to be a consensus of opinion that higher order methods for shock capturing are likely to be characterized by overshoot and oscillations behind the shock.¹³ Our results appear to be no exception. Van Leer's oscillation limiting techniques⁵ were attempted, as well as sparse use of numerical viscosity in the vicinity of the shock. For our code, the second approach seemed to give as good results as the first. Here, the Riemann solver provides a shock Mach number, which is a maximum at the point of inflection occurring within the structure of the physical shock. This provided a means for limiting application of artificial viscosity, to a few points either side, but concentrated more to the upstream side of the shock. For density and velocity, the artificial viscosity was chosen as

$$V = 10^{-3} \left| \frac{P_{i+1} - 2P_i + P_{i-1}}{P_{i+1} + 2P_i + P_{i-1}} \right| \{V_{i+1} - 2V_i + V_{i-1}\}; \quad (26)$$

13. J. L. Steger, private communication.

The results of Figures 7-10 are calculated with this dissipation, which is of the order

$$V = 0 \left(10^{-6} \frac{\partial^2 V}{\partial R^2} \right). \quad (27)$$

The effects seem to be a dampening of oscillations behind the shock, with no apparent degradation in crispness. However, the overshoot appears to persist, about 3% in error.

In order to see that the shock is propagating properly, the calculation with the second-order method has been allowed to continue to time $t = .14$. As reported by Miner and Skop,¹¹ at this time the shock front should have progressed to $R = .75$. Figures 11-12 verify that the shock front is approximately at this location.

V. SUMMARY AND CONCLUSIONS

First and second-order accurate Godunov methods for the numerical solution of ideal compressible flows with embedded shock waves have been formulated, programmed, and tested by means of a linear shock tube calculation. Results show an immediate improvement of the crispness in shock structure, for the higher order accurate method. The higher order method appears to have inherent overshoot at the shock, together with oscillations behind the shock. It appears mandatory to dampen these oscillations, by means of Van Leer-type oscillation limiting schemes, or else through addition of artificial viscosity restricted to a small region behind the shock. Surprisingly enough, for the present problem both schemes were found to give comparable results in this respect.

Perhaps we should mention how the present method differs from Van Leer's original version,⁵ aside from the conversion to Eulerian fluid dynamics. Major differences are:

- a. Omission of some near-shock terms from Equations (23-24), heuristically added, perhaps to insure entropy increase at the shock.
- b. Use of Godunov's original nonlinear iteration scheme (References 2, 12) for the Riemann problem, versus Van Leer's more elaborate accelerated version. Although slower computationally, this scheme does distinguish between shock and compression waves; hence, it should be more accurate, as evidenced by the omission of (a).
- c. For the Lagrangean formulation, the contact surface in the Riemann problem lies along the cell interface. Hence, it is reasonable for Van Leer to employ separate left and right density $\rho_{i\pm}$ in calculating $\bar{\rho}_R$. However,

for the Euler version this practice does not appear as logical, since the contact surface can lie on either side of the cell interface. The result, and possibly the biggest drawback of the Euler version, is that contact surface resolution does not much improve, when going over to second-order accuracy.

LRAPICY2

MACH CONTOURS

20 STEPS TIME = 64.6 μ s
MIN = .40 MAX = 2.60 INC = .2000

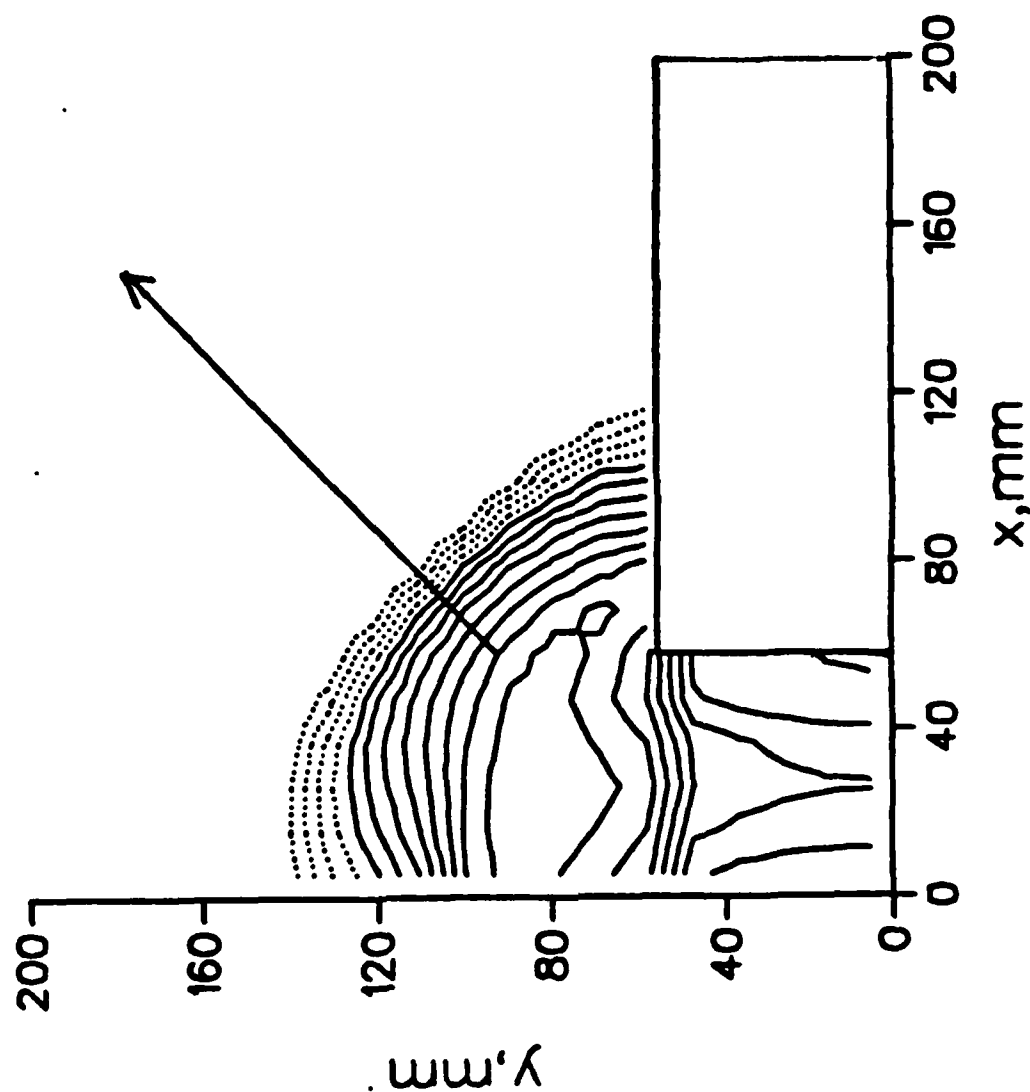


Figure 1. Two-Dimensional, Axis-Symmetric Muzzle Blast Calculation

MACH NUMBER ON RAY AXI-SYMMETRIC 1ST ORDER GODUNOV

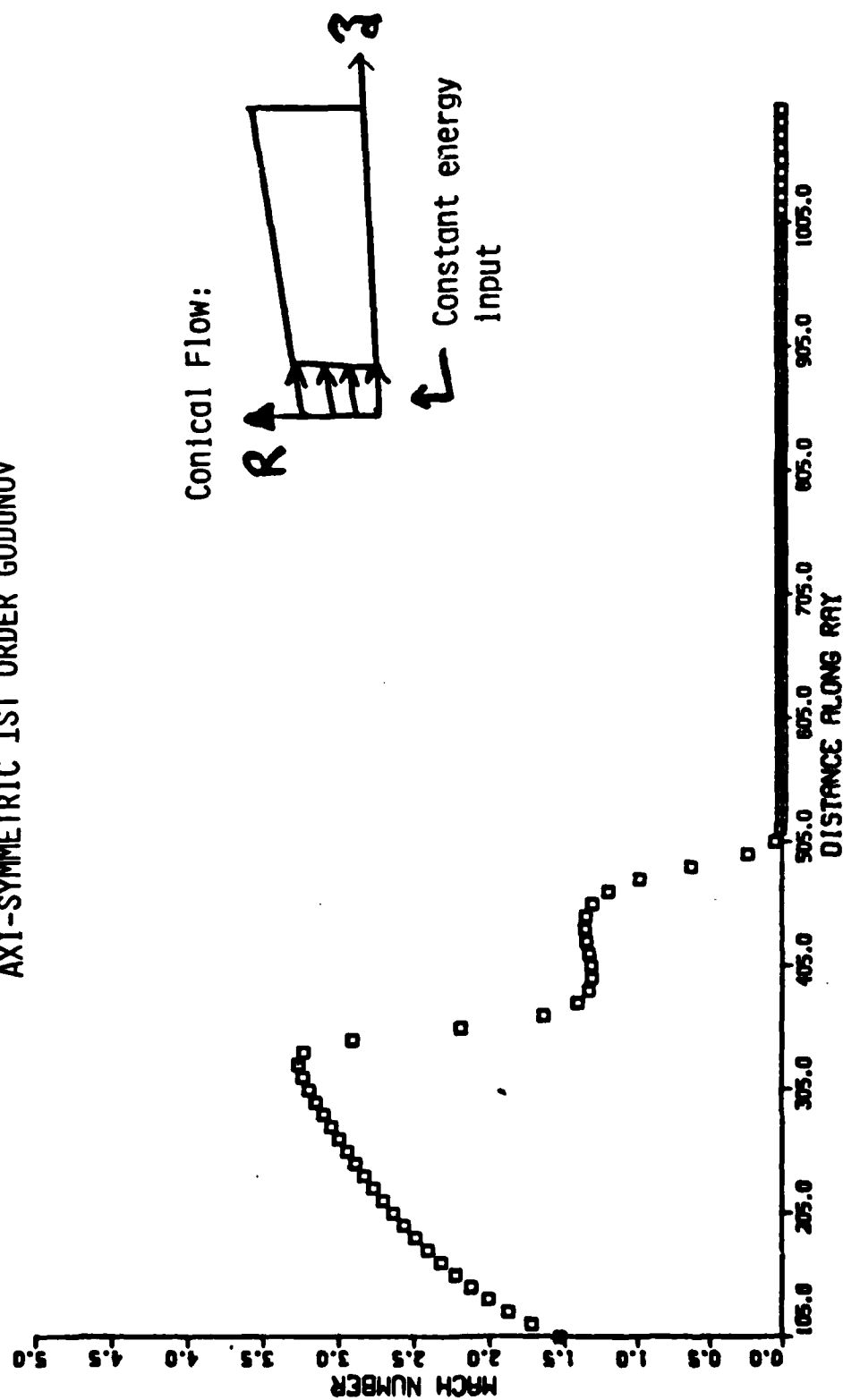


Figure 2. Shock Smearing Typical of a First Order Accurate Godunov Calculation

STREAMWISE PRESSURE
TIME - 0.659490 $\times 10^{-4}$

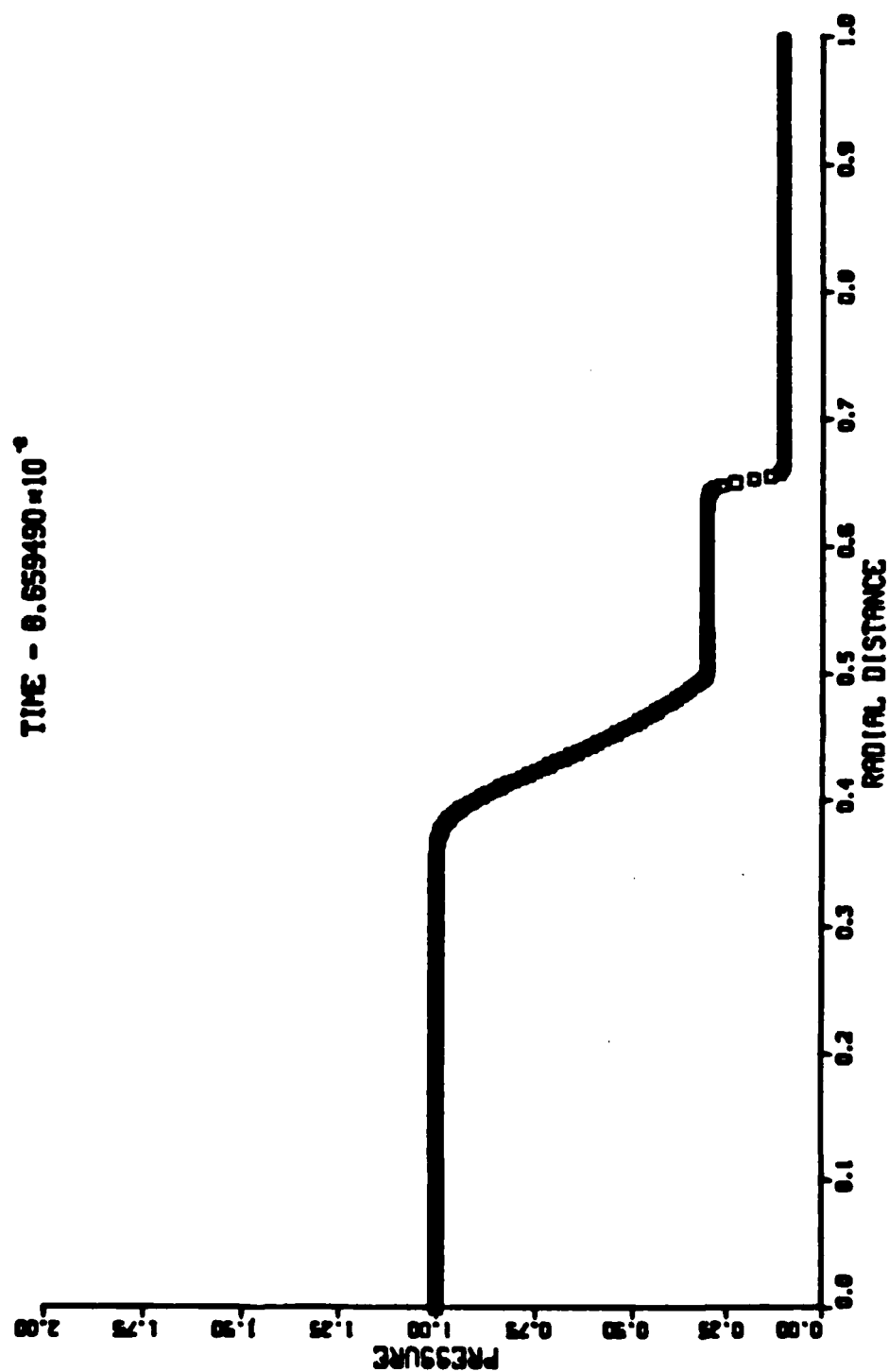


Figure 3. First Order Godunov Calculation

MACH NUMBER

TIME - 0.659490×10^{-4}

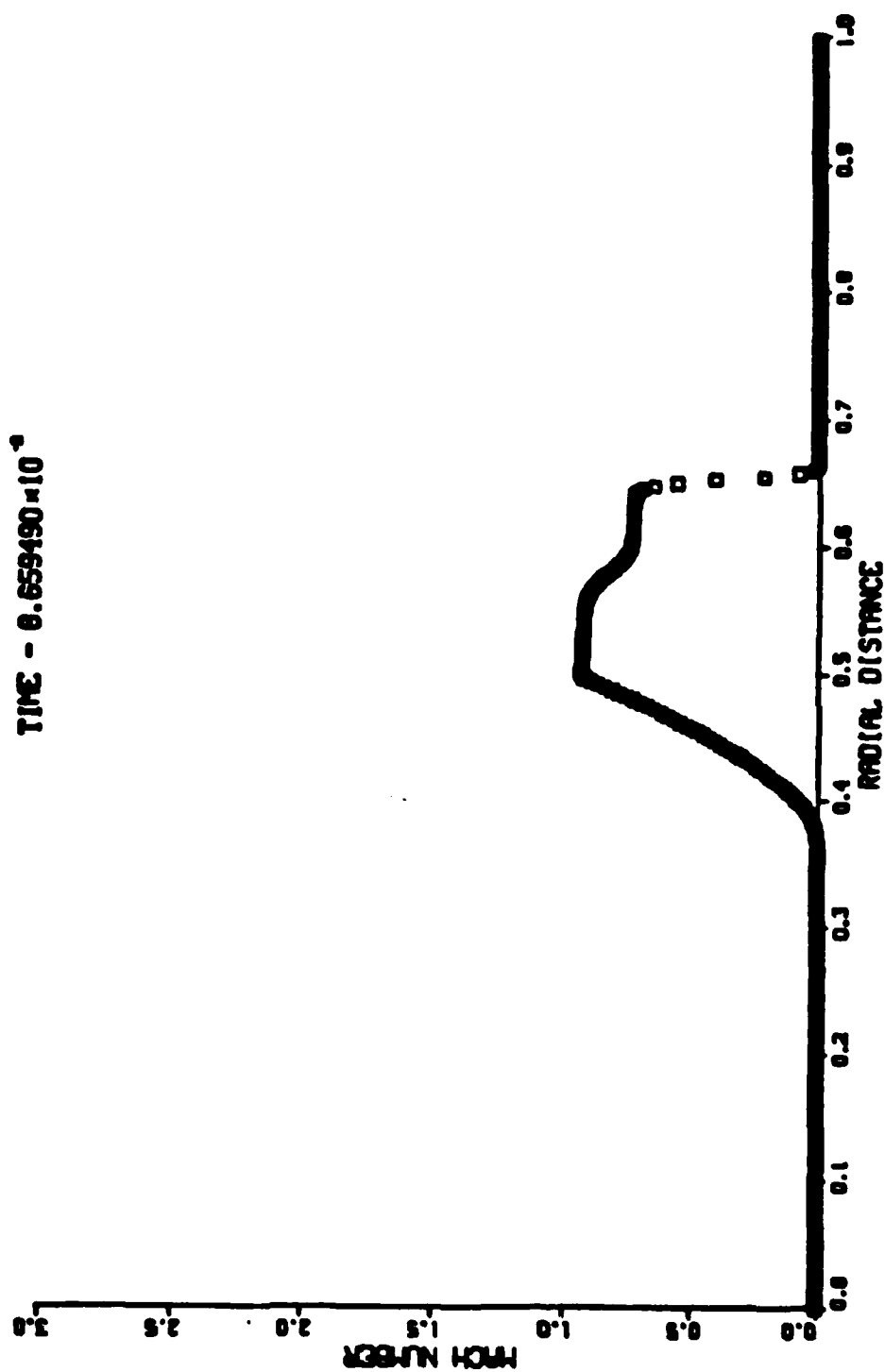


Figure 4. First Order Godunov Calculation

STREAMWISE DENSITY
TIME - 0.659490×10^{-3}

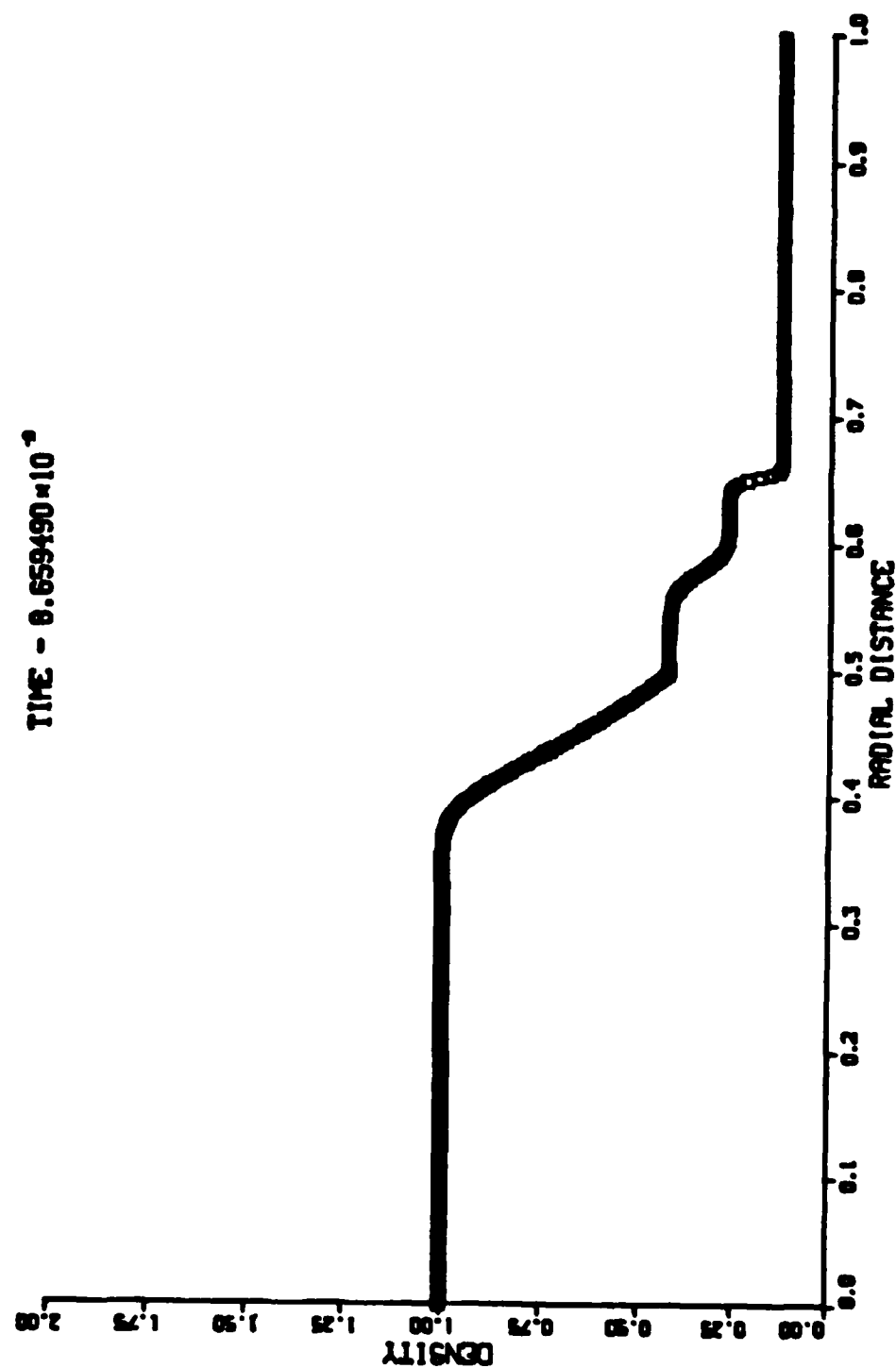


Figure 5. First Order Godunov Calculation

TOTAL VELOCITY

TIME - 0.659490×10^{-4}

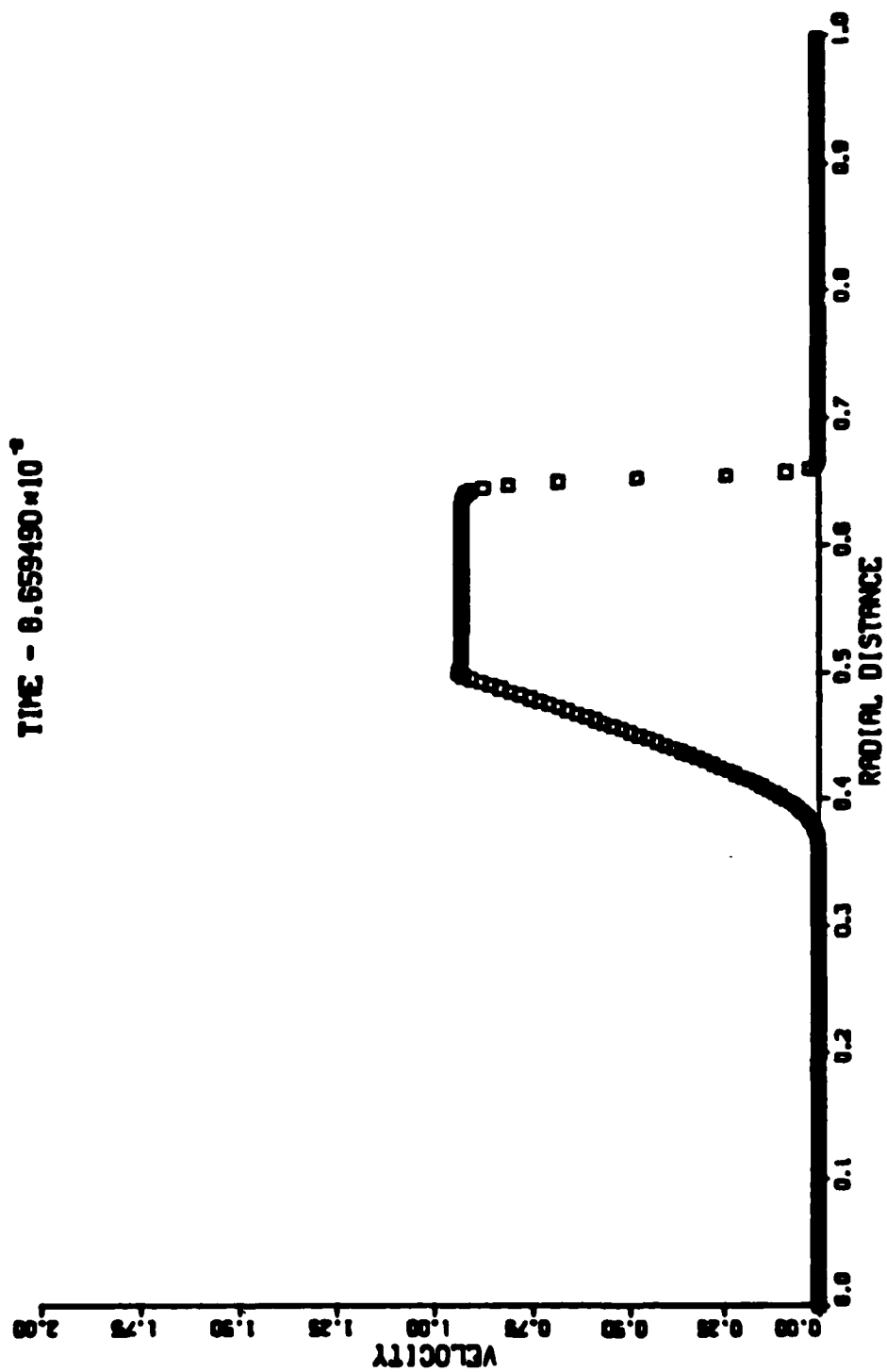


Figure 6. First Order Godunov Calculation

STREAMWISE PRESSURE

TIME - 1.149010×10^{-4}

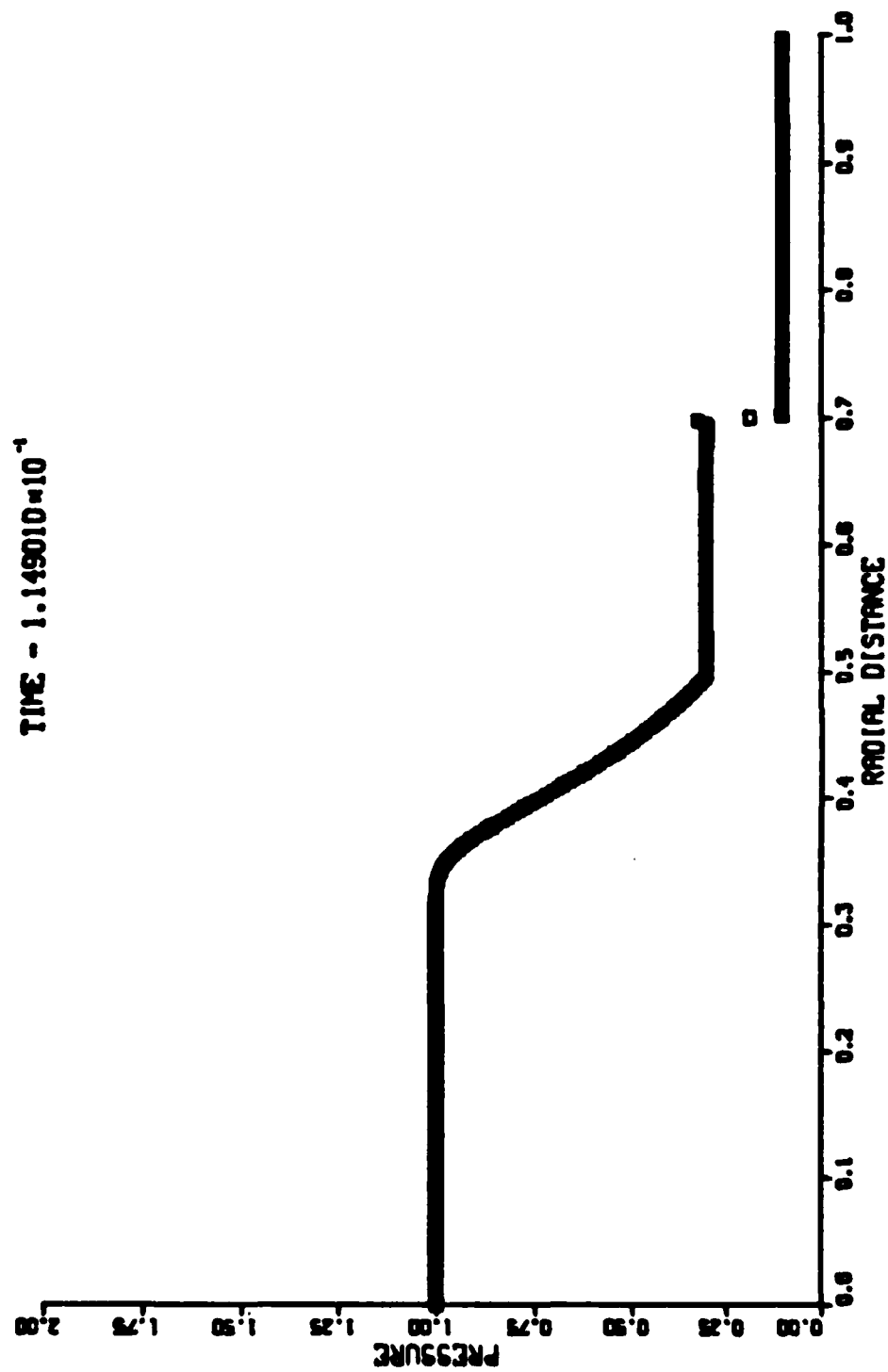


Figure 7. Second Order Godunov Calculation

MACH NUMBER

TIME - 1.149010×10^{-1}

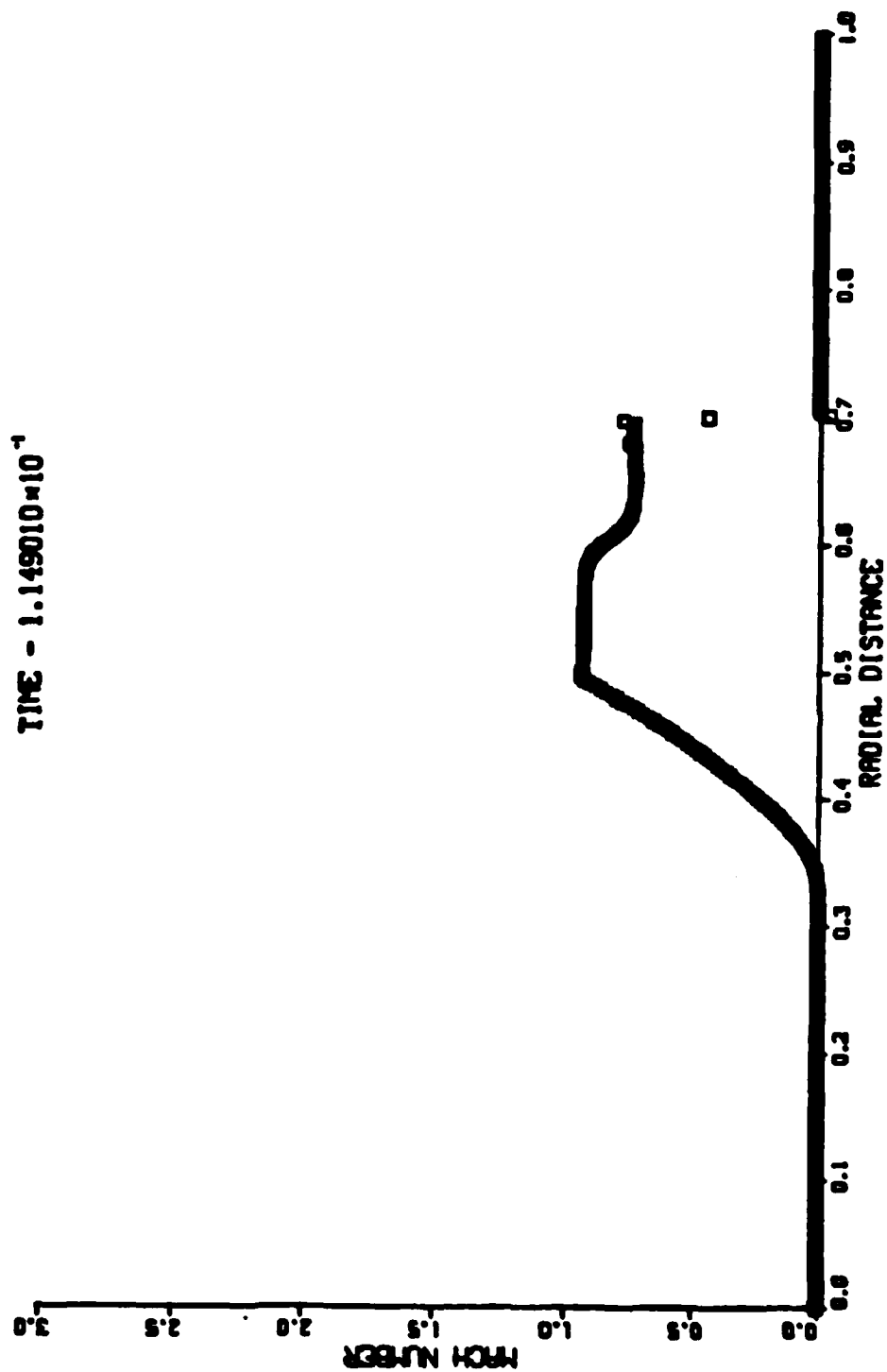


Figure 8. Second Order Godunov Calculation

STREAMWISE DENSITY

TIME - 1.149010×10^{-1}

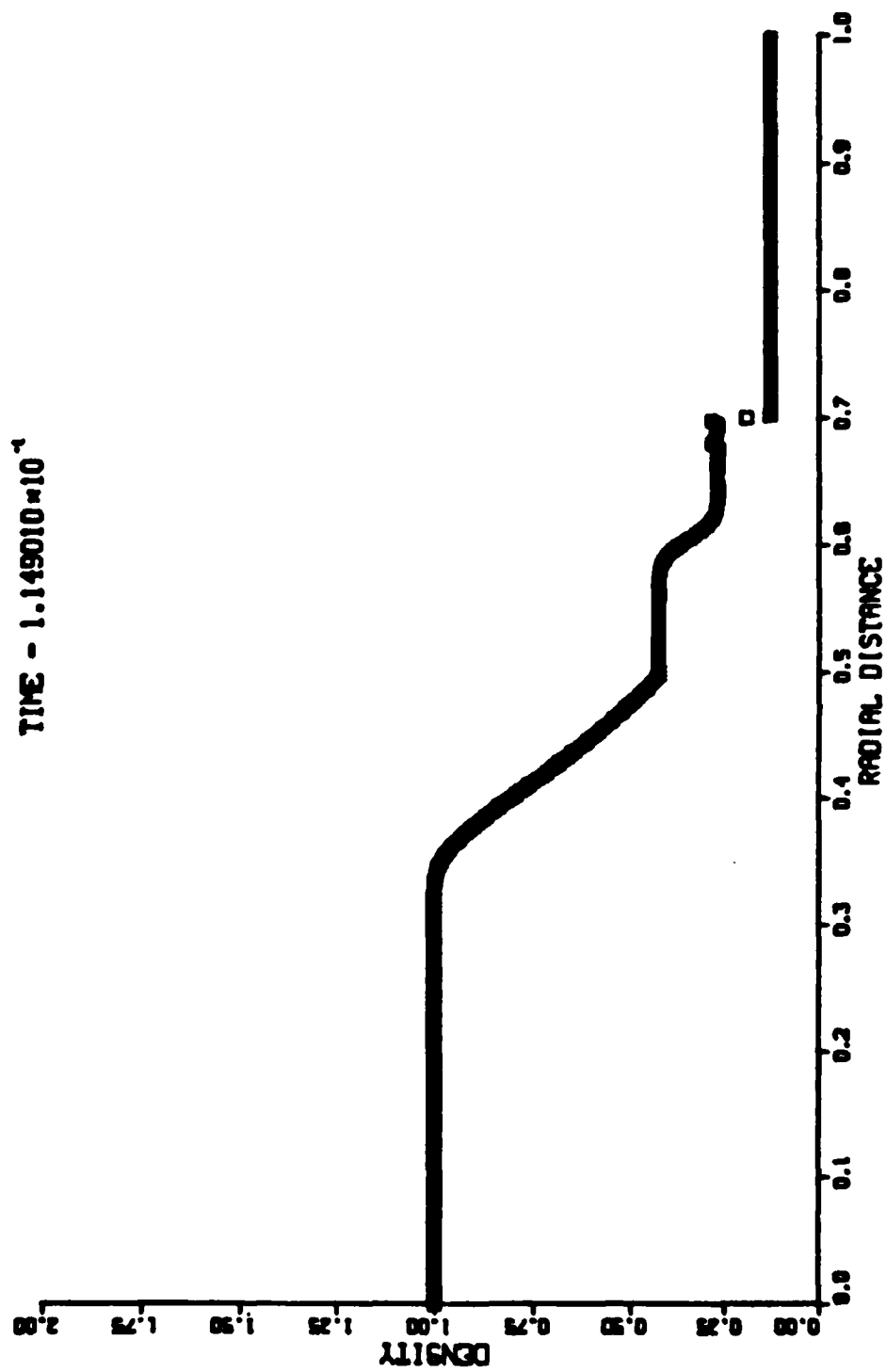


Figure 9. Second Order Godunov Calculation

TOTAL VELOCITY
TIME - 1.149010×10^{-1}

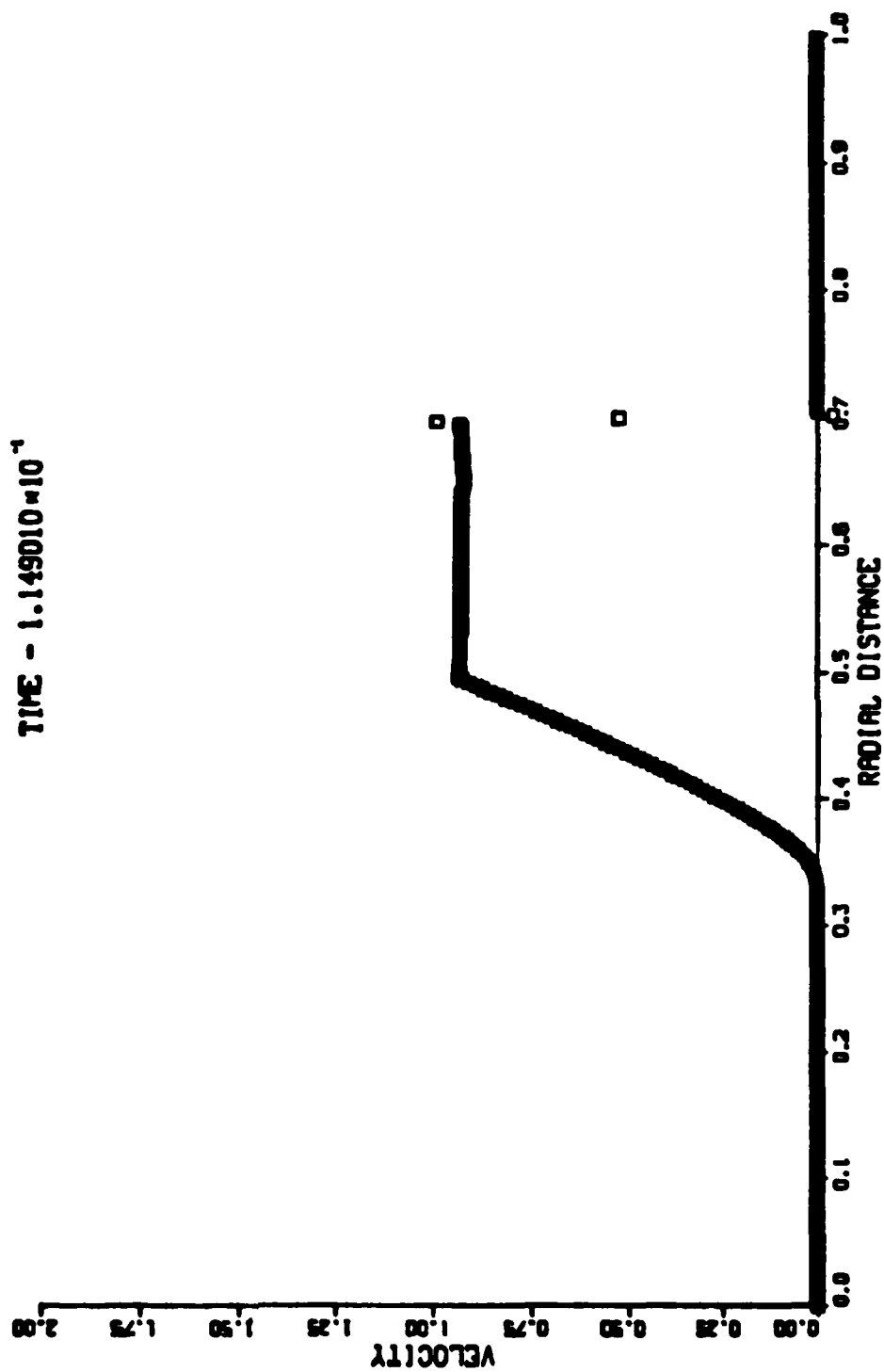


Figure 10. Second Order Godunov Calculation

STREAMWISE PRESSURE

TIME - 1.408650×10^{-1}

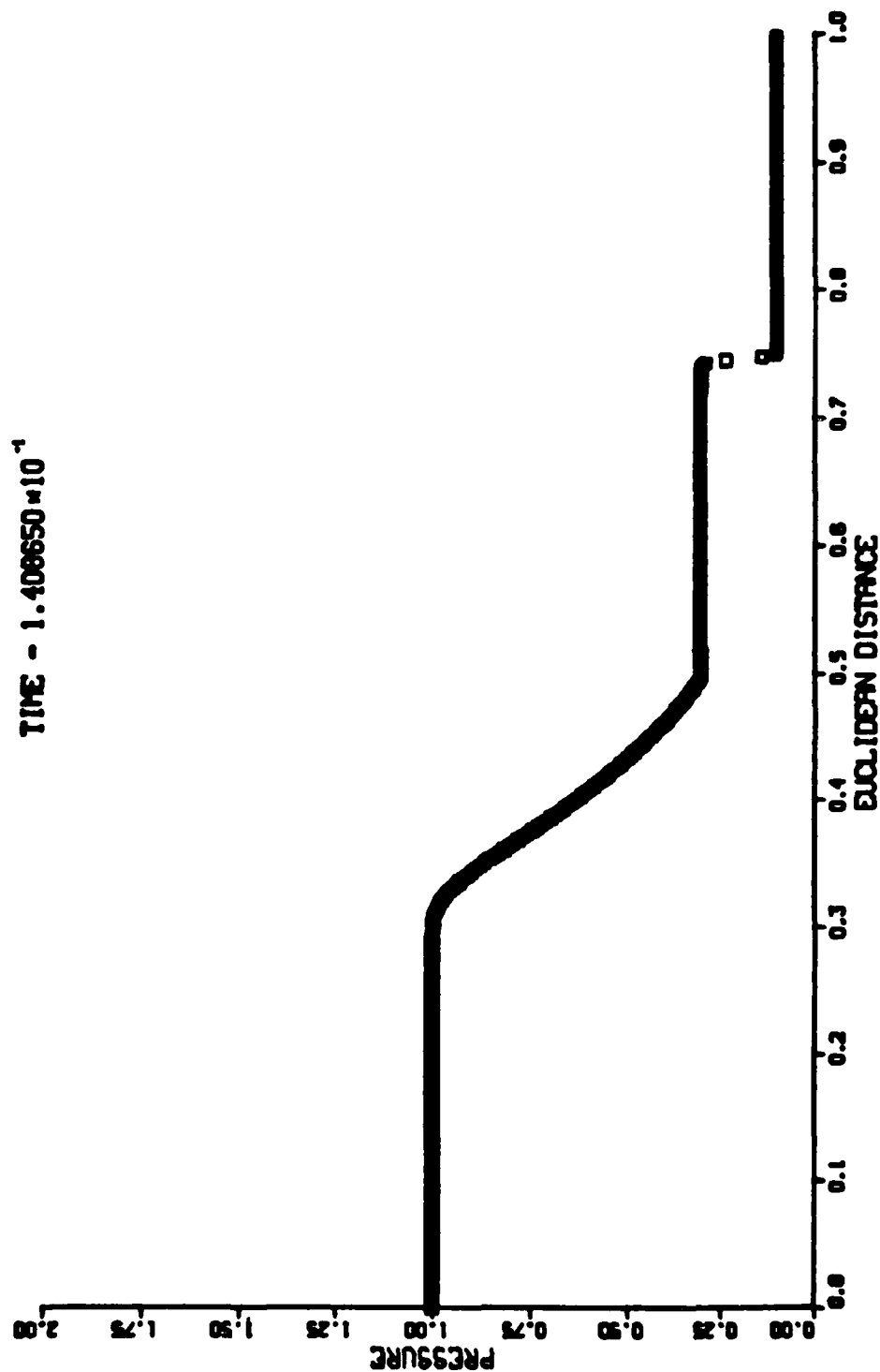


Figure 11. Progression of Pressure Jump, Second Order Godunov

TOTAL VELOCITY

TIME - 1.4048860×10^{-1}

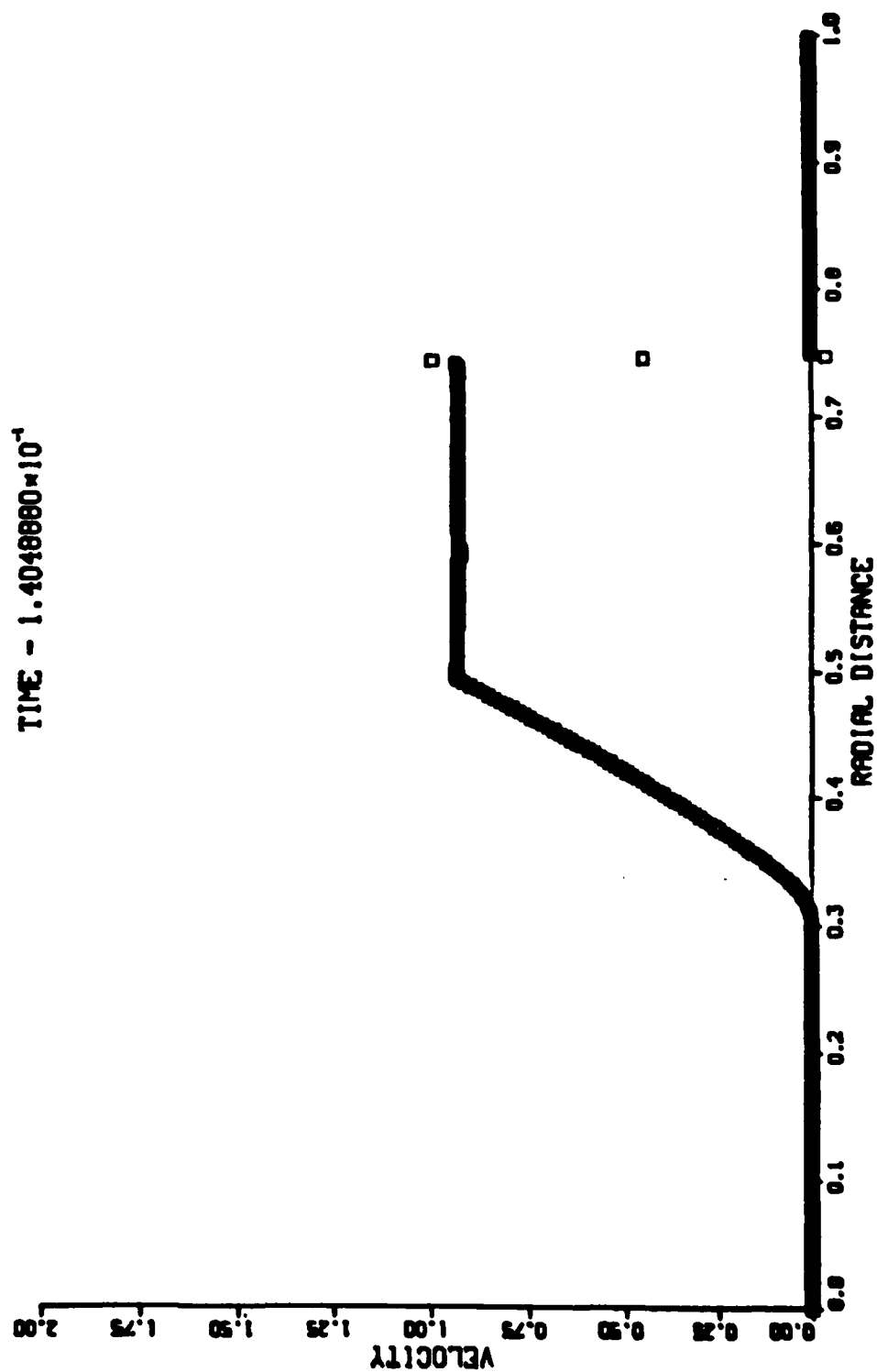


Figure 12. Progression of Velocity Jump, Second Order Godunov

REFERENCES

1. G. E. Widhopf, J. C. Buell, and E. M. Schmidt, "Time Dependent Near-Field Muzzle Brake Simulations," AIAA-82-0973, AIAA/ASME 3rd Joint Thermophysics, Fluids and Heat Transfer Conference, St. Louis, Missouri, June 1982.
2. A. M. Godunov, A. V. Zabrodin, and G. P. Prokopov, "Difference Schemes for Two-Dimensional, Unsteady Problems in Gas Dynamics and Calculation of Flows With a Detached Shock Wave," Journal of Computing Mathematics and Mathematical Physics. USSR Academy of Sciences, Vol. 1, No. 6, November-December 1961. (Translation)
3. M. L. Bundy, "A Nonsimilar Solution for Blast Waves Driven by An Asymptotic Piston Expansion," AIAA-83-0496, AIAA 21st Aerospace Sciences Meeting, January 1983, Reno, Nevada and U. S. Army Ballistic Research Laboratory, Aberdeen Proving Ground, MD, BRL Technical Report ARBRL-TR 02497, June 1983. (AD A130012)
4. M. L. Bundy, C. H. Cooke, and E. M. Schmidt, "Reshaping an Artificially Diffused Shock Solution," BRL Report, to be published.
5. B. Van Leer, "Towards The Ultimate Conservative Difference Scheme. V. A Second-Order Sequel to Godunov's Method," Journal of Computational Physics, Vol. 32, pp. 101-136, 1979.
6. P. Colella, "A Direct Eulerian MUSCL Scheme For Gas Dynamics," Lawrence Berkeley Laboratory Report LBL-14104, February 1982.
7. J. L. Steger and W. F. Warming, "Flux Vector Splitting of the Inviscid Gas Dynamics Equations with Application To Finite Difference Methods," Journal of Computational Physics, Vol. 40, No. 2, April 1981.
8. G. Moretti, "The λ Scheme," Computers and Fluids, Vol. 7, pp. 191-205, Pergamon Press, 1979.
9. H. C. Yee and R. J. Warming, "Implicit Total Variation Diminishing Schemes For Steady Flow Calculations," AIAA-83-1902, AIAA 6th Computational Fluid Dynamics Conference, Danvers, Massachusetts, July 1983.
10. G. A. Sod, "A Survey of Several Finite Difference Methods For Systems of Hyperbolic Conservation Laws," Journal of Computational Physics, Vol. 27, pp. 1-31, 1978.
11. E. W. Miner and R. A. Skop, "Explicit Time Integration For The Finite Element Shock Wave Equations," AIAA-82-0994, ASME/AIAA 3rd Joint Thermophysics, Fluids, Plasma and Heat Transfer Conference, St. Louis, Missouri, June 1982.

REFERENCES (continued)

12. M. Holt, Numerical Fluid Dynamics, Springer-Verlag, Berlin, Heidelberg, New York, 1977.
13. J. L. Steger, private communication.

DISTRIBUTION LIST

<u>No. of Copies</u>	<u>Organization</u>	<u>No. of Copies</u>	<u>Organization</u>
12	Administrator Defense Technical Info Center ATTN: DTIC-DDA Cameron Station Alexandria, VA 22314	1	President US Army Aviation Test Board ATTN: ATZQ-OP-AA Ft. Rucker, AL 36360
1	Commander US Army Materiel Command ATTN: AMCDRA-ST 5001 Eisenhower Avenue Alexandria, VA 22333	1	Commander US Army Medical Research and Development Command ATTN: SGRD-ZBM-C/LTC Lamothe Ft. Detrick, MD 21701
1	Commander US Army Materiel Command ATTN: AMCDL 5001 Eisenhower Avenue Alexandria, VA 22333	1	Commander US Army Communications Resch and Development Command ATTN: AMSEL-ATDD Fort Monmouth, NJ 07703
1	Commander US Army Materiel Command ATTN: AMCDE-R, Lockert 5001 Eisenhower Avenue Alexandria, VA 22333	1	Commander US Army Missile Command ATTN: AMSMI-R Redstone Arsenal, AL 35898
4	Commander US Army Aviation Research and Development Command ATTN: Tech Dir (Mr. R. Lewis) AMSAV -E AMCPM-AAH (Mr. Corgiatt) Product Manager, AH-1 4300 Goodfellow Boulevard St. Louis, MO 63120	1	Commander US Army Missile Command ATTN: AMSMI-RBL Redstone Arsenal, AL 35898
1	Director US Army Air Mobility Research and Development Laboratory Ames Research Center Moffett Field, CA 94035	1	Commander US Army Missile Command ATTN: AMSMI-TLH Redstone Arsenal, AL 35898
1	Commander US Army Electronics Research and Development Command Technical Support Activity ATTN: AMDSD-L Fort Monmouth, NJ 07703	1	Commander US Army Missile Command ATTN: AMSMI-RDK Redstone Arsenal, AL 35898
		1	Commander US Army Missile Command ATTN: AMSMI-YDL Redstone Arsenal, AL 35898
		1	Commander US Army Tank Automotive Command ATTN: AMSTA-TSL Warren, MI 48090

DISTRIBUTION LIST (Continued)

<u>No. of Copies</u>	<u>Organization</u>	<u>No. of Copies</u>	<u>Organization</u>
1	Commander US Army Armament Munitions & Chemical Command ATTN: AM SMC-LEP-L(R) Rock Island, IL 61299	1	Commander US Army Jefferson Proving Ground Madison, IN 47251
7	Commander Armament R&D Center US Army AMCCOM ATTN: SMCAR-TSS SMCAR-TDS, Mr. Lindner SMCAR-LC-F, Mr. Loeb SMCAR-LCW, Mr. M. Salsbury SMCAR-LCW, Mr. R. Wrenn SMCAR-CAWS, Mr. Barth SMCAR-SEM, W. Bielauskas Dover, NJ 07801	1	Commander US Army Materials and Mechanics Research Center ATTN: AM XMR-ATL Watertown, MA 02172
1	ODCSI, USAREUR & 7A ATTN: AEAGB-PDN(S&E) APO, NY 09403	1	Commander US Army Natick Research and Development Laboratory ATTN: DRDNA, Dr. D. Sieling Natick, MA 01760
1	Director Division of Medicine WRAIR/WRAMC ATTN: SGRD-UWH-D/MAJ Jaeger Washington, DC 20012	1	Commander US Army Aeromedical Research Laboratory ATTN: SGRD-UAH-AS, Dr. Patterson P.O. Box 577 Ft. Rucker, AL 36360
6	Commander Armament R&D Center US Army AMCCOM ATTN: SMCAR-LCV, Mr. Reisman SMCAR-SCA, Mr. Kahn SMCAR-LC, Dr. Frasier SMCAR-SCW, Mr. Townsend SMCAR-TDC, Dr. Gyorog SMCAR-SG, Dr. T. Hung Dover, NJ 07801	1	Director US Army TRADOC Systems Analysis Activity ATTN: ATAA-SL White Sands Missile Range NM 88002
4	Director Benet Weapons Laboratory Armament R&D Center US Army AMCCOM ATTN: SMCAR-LCB-TL CPT R. Dillon Dr. G. Carofano Dr. C. Andrade Watervliet, NY 12189	1	Commandant US Army Infantry School ATTN: ATSH-CD-CSO-OR Ft. Benning, GA 31905
1	HQDA AMA-ART-M Washington, DC 20310	1	Commander US Army Research Office ATTN: CRD-AA-EH P.O. Box 12211 Research Triangle Park NC 27709
		1	Commander US Army Ballistic Missile Defense Systems Command P.O. Box 1500 Huntsville, AL 35807
		1	Commander US Army Development & Employment Agency ATTN: MODE-TED-SAB Fort Lewis, WA 98433

DISTRIBUTION LIST (Continued)

<u>No. of Copies</u>	<u>Organization</u>	<u>No. of Copies</u>	<u>Organization</u>
3	Commander Naval Air Systems Command ATTN: AIR-604 Washington, DC 20360	2	AFATL (DLRA, F. Burgess; Tech Lib) Eglin AFB, FL 32542
3	Commander Naval Sea Systems Cmd Washington, DC 20360	1	AFWL/SUL Kirtland AFB, NM 87117
2	Commander David W. Taylor Naval Ship Research & Development Ctr ATTN: Lib Div, Code 522 Aerodynamic Lab Bethesda, MD 20084	1	ASD/XRA (Stinfo) Wright-Patterson AFB, OH 45433
4	Commander Naval Surface Weapons Center ATTN: 6X Mr. F. H. Maille Dr. J. Yagla Dr. G. Moore Dahlgren, VA 22448	1	Director National Aeronautics and Space Administration George C. Marshall Space Flight Center ATTN: MS-I, Lib Huntsville, AL 38512
1	Commander Naval Surface Weapons Center ATTN: Code 730 Silver Spring, MD 20910	1	Director Jet Propulsion Laboratory ATTN: Tech Lib 4800 Oak Grove Drive Pasadena, CA 91109
1	Commander Naval Weapons Center ATTN: Code 553, Tech Lib China Lake, CA 93555	1	Director NASA Scientific & Technical Information Facility ATTN: SAK/DL P.O. Box 8757 Baltimore/Washington International Airport, MD 21240
1	Commander Naval Weapons Center ATTN: Tech Info Div Washington, DC 20375	1	AAI Corporation ATTN: Dr. T. Stastny P.O. Box 126 Cockeysville, MD 21030
1	Commander Naval Ordnance Station ATTN: Code FS13A, P. Sewell Indian Head, MD 20640	1	Advanced Technology Labs ATTN: Mr. J. Erdos Merrick & Steward Avenues Westbury, NY 11590
		1	Aerospace Corporation ATTN: Dr. G. Widhopf P.O. Box 92957 Los Angeles, CA 90009

DISTRIBUTION LIST (Continued)

<u>No. of Copies</u>	<u>Organization</u>	<u>No. of Copies</u>	<u>Organization</u>
1	ARTEC Associates, Inc. ATTN: Dr. S. Gill 26046 Eden Landing Road Hayward, CA 94545	1	Olin Corporation 275 Winchester Avenue New Haven, CT 06504
1	AVCO Systems Division ATTN: Dr. D. Siegelman 201 Lowell Street Wilmington, MA 01887	1	Director Sandia National Laboratory ATTN: Aerodynamics Dept Org 5620, R. Maydew Albuquerque, NM 87115
1	Battelle Columbus Laboratories ATTN: D.J. Butz 505 King Avenue Columbus, OH 43201	1	Guggenheim Aeronautical Lab California Institute of Tech ATTN: Tech Lib Pasadena, CA 91104
1	Technical Director Colt Firearms Corporation 150 Huyshope Avenue Hartford, CT 14061	1	Franklin Institute ATTN: Tech Lib Race & 20th Streets Philadelphia, PA 19103
1	ARO, Inc Von Karman Gasdynamics Facility ATTN: Dr. J. Lewis Arnold AFS, TN 37389	1	Director Applied Physics Laboratory The Johns Hopkins University John Hopkins Road Laurel, MD 20707
1	General Electric Corporation Armaments Division ATTN: Mr. R. Whyte Lakeside Avenue Burlington, VT 05401	1	Massachusetts Institute of Technology Dept of Aeronautics and Astronautics ATTN: Tech Lib 77 Massachusetts Avenue Cambridge, MA 02139
1	Honeywell, Inc. ATTN: Mail Station MN 112190 (G. Stilley) 600 Second Street, North East Hopkins, MN 55343	1	Ohio State University Dept of Aeronautics and Astronautical Engineering ATTN: Tech Lib Columbus, OH 43210
1	Hughes Helicopter Company Bldg. 2, MST22B ATTN: Mr. R. Forker Centinella and Teale Streets Culver City, CA 90230	3	Polytechnic Institute of New York Graduate Center ATTN: Tech Lib Prof. S. Lederman Prof. R. Cresci Route 110 Farmingdale, NY 11735
1	Martin Marietta Aerospace ATTN: Mr. A. J. Culotta P.O. Box 5837 Orlando, FL 32805		

DISTRIBUTION LIST (Continued)

<u>No. of Copies</u>	<u>Organization</u>	<u>Aberdeen Proving Ground</u>
1	Director Forrestal Research Center Princeton University Princeton, NJ 08540	Dir, USAMSAA ATTN: AMXSY-D AMXSY-MP, H. Cohen
1	Kaman Tempo ATTN: Mr. J. Hindes 816 State Street P.O. Drawer QQ Santa Barbara, CA 93102	Cdr, USATECOM ATTN: AMSTE-TO-F
1	Southwest Research Institute ATTN: Mr. Peter S. Westine P.O. Drawer 28510 8500 Culebra Road San Antonio, TX 78228	Cdr, CRDC, AMCCOM ATTN: SMCCR-RSP-A SMCCR-MU SMCCR-SPS-IL
2	Boeing Aerospace Corporation ATTN: C. R. Pond P. D. Texeira MS 8C-64 PO Box 3999 Seattle, WA 98124	Dir, Wpns Sys Concepts Team ATTN: SMCCR -ACW
		Dir, USAHEL ATTN: Dr. Weisz Dr. Cummings Mr. Garinther
		Cdr, CSTA ATTN: Mr. S. Walton

USER EVALUATION SHEET/CHANGE OF ADDRESS

This Laboratory undertakes a continuing effort to improve the quality of the reports it publishes. Your comments/answers to the items/questions below will aid us in our efforts.

1. BRL Report Number _____ Date of Report _____
2. Date Report Received _____
3. Does this report satisfy a need? (Comment on purpose, related project, or other area of interest for which the report will be used.) _____

4. How specifically, is the report being used? (Information source, design data, procedure, source of ideas, etc.) _____

5. Has the information in this report led to any quantitative savings as far as man-hours or dollars saved, operating costs avoided or efficiencies achieved, etc? If so, please elaborate. _____

6. General Comments. What do you think should be changed to improve future reports? (Indicate changes to organization, technical content, format, etc.) _____

CURRENT ADDRESS

Name _____

Organization _____

Address _____

City, State, Zip _____

7. If indicating a Change of Address or Address Correction, please provide the New or Correct Address in Block 6 above and the Old or Incorrect address below.

OLD ADDRESS

Name _____

Organization _____

Address _____

City, State, Zip _____

(Remove this sheet along the perforation, fold as indicated, staple or tape closed, and mail.)

----- FOLD HERE -----

Director
US Army Ballistic Research Laboratory
ATTN: AMXBR-OD-ST
Aberdeen Proving Ground, MD 21005-5066

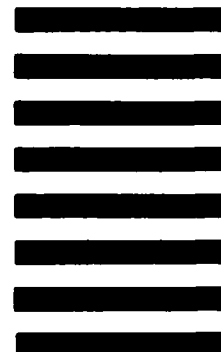


NO POSTAGE
NECESSARY
IF MAILED
IN THE
UNITED STATES

OFFICIAL BUSINESS
PENALTY FOR PRIVATE USE, \$300

BUSINESS REPLY MAIL
FIRST CLASS PERMIT NO 12062 WASHINGTON, DC
POSTAGE WILL BE PAID BY DEPARTMENT OF THE ARMY

Director
US Army Ballistic Research Laboratory
ATTN: AMXBR-OD-ST
Aberdeen Proving Ground, MD 21005-9989



----- FOLD HERE -----

END

FILMED

1-85

DTIC